Inorg. Chem. **2006**, *45*, 6411–6423

Synthesis, Structures, and Olefin Polymerization Capability of Vanadium(4+) Imido Compounds with *fac*-N_3 Donor Ligands

Helen R. Bigmore,[†] Martin A. Zuideveld,[‡] Radoslaw M. Kowalczyk,[§] Andrew R. Cowley,[†] Mirko Kranenburg,[||] Eric J. L. McInnes,[§] and Philip Mountford*,[†]

Chemistry Research Laboratory, University of Oxford, Mansfield Road, Oxford OX1 3TA, U.K., DSM Research, P.O. Box 18, 6160 MD Geleen, The Netherlands, EPSRC c. w. EPR Service Centre, School of Chemistry, The University of Manchester, Oxford Road, Manchester M13 9PL, U.K., and DSM Elastomers, Global R&D, P.O. Box 1130, 6160 BC Geleen, The Netherlands

Received March 16, 2006

One-pot reactions of $V(NMe_2)_4$ with a range of primary alkyl- and arylamines RNH_2 and Me_3SiCl afforded the corresponding five-coordinate vanadium(4+) imido compounds $V(NR)Cl_2(NHMe_2)_2$ [R = 2,6-$C_6H_3{}^iPr_2$ (**1a**, previously reported), 2-$C_6H_4{}^tBu$ (**1b**), 2-$C_6H_4CF_3$ (**1c**), ^tBu (**1d**), Ad (Ad = adamantyl, **1e**)]. The crystal structures of **1b** (two diamorphic forms) and **1c** featured N–H···Cl hydrogen-bonded chains. Reaction of **1a**–**e** with the neutral face-capping, N_3 donor ligands TACN (TACN = 1,4,7-trimethyltriazacyclononane) or TPM [TPM = tris(3,5-dimethylpyrazolyl)methane] gave the corresponding six-coordinate complexes $V(NR)(TACN)Cl_2$ (**2a**–**e**) and $V(NR)(TPM)Cl_2$ (**3a**–**e**). The X-ray structures of **2b**, **2c**, **2d**, **3b**, **3c**, and **3e** were determined. When activated with methylaluminoxane, certain of the complexes $V(NR)(TPM)Cl_2$ (**3**) formed moderately active ethylene polymerization catalysts, whereas none of the compounds $V(NR)(TACN)Cl_2$ (**2**) were active.

Introduction

Among the many types of homogeneous non-cyclopentadienyl Ziegler−Natta polymerization catalysts,[1−7] imido compounds (bearing the formally dianionic NR^{2-} ligand) have also been of interest.[8] Starting from the versatile synthons $Ti(NR)Cl_2(NHMe_2)_2$ (**I**;[9] Chart 1), we recently prepared and evaluated two titanium(4+) imido catalyst families of the types $Ti(NR)(TACN)Cl_2$ (**II**, where TACN = 1,4,7-trimethyltriazacyclononane; Chart 1)[10] and $Ti(NR)(TPM)Cl_2$ [**III**, where TPM = tris(3,5-dimethylpyrazolyl)methane].[11] When activated with methylaluminoxane (MAO), some of the compounds **II** and **III** were the most productive imido-based ethylene homopolymerization precatalysts reported to date (productivities of up to ca. 10^3 kg mol^{-1} h^{-1} bar^{-1} at ambient temperature and ca. 10^5 kg mol^{-1} h^{-1} bar^{-1} at 100 °C). Interestingly, the two different classes of catalysts showed a quite different dependence of productivity on the imido nitrogen substituent, especially at higher temperatures. The TACN-supported systems showed the highest productivities when the N−R substituent was a bulky alkyl group [^tBu, $CMe_2CH_2{}^tBu$, or adamantyl (Ad)], whereas the TPM-supported systems were much less active for these substituents and showed their highest productivities for bulky ortho-substituted aryl groups (e.g., 2-$C_6H_4{}^tBu$, 2-$C_6H_4CF_3$, and 2,6-$C_6H_3{}^iPr_2$). This has been attributed to the topological

* To whom correspondence should be addressed. E-mail: philip.mountford@chem.oxford.ac.uk (P.M.).
[†] University of Oxford.
[‡] DSM Research.
[§] The University of Manchester.
[||] DSM Elastomers.

(1) Britovsek, G. J. P.; Gibson, V. C.; Wass, D. F. *Angew. Chem., Int. Ed.* **1999**, *38*, 429.
(2) Ittel, S. D.; Johnson, L. K.; Brookhart, M. *Chem. Rev.* **2000**, *100*, 1169.
(3) Piers, W. E.; Emslie, D. J. H. *Coord. Chem. Rev.* **2002**, *233−234*, 131.
(4) Gibson, V. C.; Spitzmesser, S. K. *Chem. Rev.* **2003**, *103*, 283.
(5) Suzuki, Y.; Terao, H.; Fujita, T. *Bull. Chem. Soc. Jpn.* **2003**, *76*, 1493.
(6) Mitani, M.; Saito, J.; Ishii, S.; Nakayama, Y.; Makio, H.; Matsukawa, N.; Matsui, S.; Mohri, J.; Furuyama, R.; Terao, H.; Bando, H. H. T.; Fujita, T. *Chem. Rec.* **2004**, *4*, 137.
(7) Stephan, D. W. *Organometallics* **2005**, *24*, 2548.
(8) Bolton, P. D.; Mountford, P. *Adv. Synth. Catal.* **2005**, *347*, 355.
(9) Adams, N.; Bigmore, H. R.; Blundell, T. L.; Boyd, C. L.; Dubberley, S. R.; Sealey, A. J.; Cowley, A. R.; Skinner, M. E. G.; Mountford, P. *Inorg. Chem.* **2005**, *44*, 2882.
(10) Adams, N.; Arts, H. J.; Bolton, P. D.; Cowell, D.; Dubberley, S. R.; Friederichs, N.; Grant, C.; Kranenburg, M.; Sealey, A. J.; Wang, B.; Wilson, P. J.; Cowley, A. R.; Mountford, P.; Schröder, M. *Chem. Commun.* **2004**, 434.
(11) Bigmore, H. R.; Dubberley, S. R.; Kranenburg, M.; Lawrence, S. C.; Sealey, A. J.; Selby, J. D.; Zuideveld, M.; Cowley, A. R.; Mountford, P. *Chem. Commun.* **2006**, 436.

10.1021/ic060454i CCC: $33.50
Published on Web 07/08/2006

Chart 1

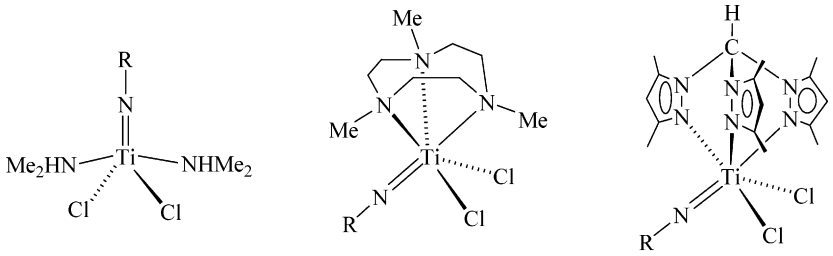

I **II** **III**

differences between the macrocyclic (TACN) and podand-like (TPM) *fac*-N_3 donor ligands.[11]

Given the excellent productivities of the titanium(4+) systems **II** and **III**, we were interested in extending these catalyst families to vanadium, a metal also of considerable interest in the context of Ziegler−Natta polymerization catalysis.[4,12,13] Imidovanadium(5+) catalysts of the type $V(NR)(L_n)X_2$ (X = halide, alkyl, or other monoanionic ligand)[8] have been known for over a decade with supporting ligands or ligand sets L_n including tris(pyrazolyl)borate,[14,15] cyclopentadienyl,[16−18] aryloxide[19−22] and ketimide.[23] In contrast to these extensive studies of imidovanadium(5+) systems, there has been only one very brief preliminary communication of vanadium(4+) imido catalysts, this being for Lorber's $V(N\text{-}2,6\text{-}C_6H_3{}^iPr_2)(X)_2(NHMe_2)_2$ (X = NMe_2 or Cl), which gave productivities of up to ca. 60 kg mol^{-1} h^{-1} bar^{-1} when activated with $EtAlCl_2$ or MAO.[24] Furthermore, vanadium(4+) Ziegler−Natta catalysts in general have not yet been extensively studied,[1,4,12,13,25−31] and there have therefore been few direct comparisons of the polymerization behavior of vanadium(4+) d^1 catalyst systems with their isostructural titanium(4+) d^0 analogues.[26,28,29]

In this paper, we describe synthetic, structural, and polymerization studies of new vanadium(4+) imido synthons of the type $V(NR)Cl_2(NHMe_2)_2$ and their TACN and TPM derivatives.

Results and Discussion

Synthesis and Solid-State Structures of New Imidobis-(dimethylamine) Compounds $V(NR)Cl_2(NHMe_2)_2$. The titanium(4+) imido catalyst families $Ti(NR)(TACN)Cl_2$ (**II**)[10] and $Ti(NR)(TPM)Cl_2$ (**III**)[11] (R = alkyl or aryl; Chart 1) were readily prepared from the desired *fac*-N_3 donor and the new imidobis(dimethylamine) precursors $Ti(NR)Cl_2(NHMe_2)_2$.[9] An analogous approach was also successful for the synthesis of a series of terminal titanium hydrazido(2−) complexes $Ti(NNPh_2)(fac\text{-}N_3)Cl_2$ from $Ti(NNPh_2)Cl_2(NHMe_2)_2$.[32] We anticipated that a similar strategy would be viable for preparing the vanadium(4+) imido analogues $V(NR)(fac\text{-}N_3)Cl_2$ (*fac*-N_3 = TACN or TPM).

Lorber et al. have recently prepared potentially suitable vanadium(4+) arylimido complexes $V(NAr)Cl_2(NHMe_2)_2$ [Ar = Ph, C_6F_5, 2,6-$C_6H_3R_2$ (R = Me, ^{i}Pr (**1a**), Cl)],[33] via "one-pot" syntheses from $V(NMe_2)_4$, $ArNH_2$, and Me_3SiCl in 73−96% yield. Pyridine, bipyridine, and tetramethylethylenediamine adducts of the $V(NR)Cl_2$ moiety were obtained from some of these complexes. However, bulky alkylimido compounds (e.g., with *tert*-butyl or Ad) were not reported, nor were arylimido compounds with larger ortho substituents (namely, *tert*-butyl and CF_3). Such substituents were the most important in the titanium imido catalyst families **II** and **III**. We therefore extended Lorber's method to prepare the homologous compounds $V(NR)Cl_2(NHMe_2)_2$ [R = 2-$C_6H_4{}^tBu$ (**1b**), 2-$C_6H_4CF_3$ (**1c**), ^{t}Bu (**1d**), or Ad (**1e**)] as green or brown air- and moisture-sensitive solids as summarized in eq 1. The arylimido compounds were obtained in somewhat higher yield (91 and 90%) than the alkylimido analogues (64 and 67%), which may reflect the differences in solubility.

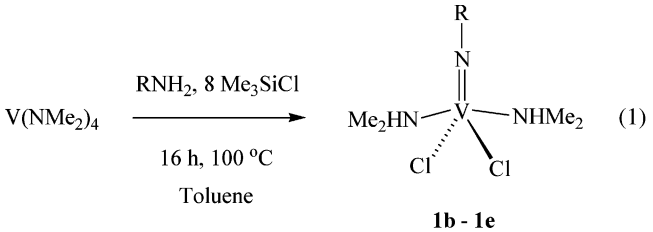

(1)

R = 2-$C_6H_4{}^tBu$ (**b**), 2-$C_6H_4CF_3$ (**c**), ^{t}Bu (**d**) or Ad (**e**)

The new compounds **1b**−**e** all feature ν(N−H) bands in their IR spectra; these data are summarized in Table 1 along

(12) Hagen, H.; Boersma, J.; van Koten, G. *Chem. Soc. Rev.* **2002**, *31*, 357.
(13) Gambarotta, S. *Coord. Chem. Rev.* **2003**, *237*, 229.
(14) Scheuer, S.; Fischer, J.; Kress, J. *Organometallics* **1995**, *14*, 2627.
(15) Casagrande, A. C. A.; Tavares, T. T. d. R.; Kuhn, M. C. A.; Casagrande, O. L.; dos Santos, J. H. Z.; Teranishi, T. *J. Mol. Catal. A* **2004**, *212*, 267.
(16) Chan, M. C. W.; Chew, K. C.; Dalby, C. I.; Gibson, V. C.; Kohlmann, A.; Little, I. R.; Reed, W. *Chem. Commun.* **1998**, 1673.
(17) Coles, M. P.; Dalby, C. I.; Gibson, V. C.; Little, I. R.; Marshall, E. L.; Ribeiro da Costa, M. H.; Mastroianni, S. *J. Organomet. Chem.* **1999**, *591*, 78.
(18) Sato, Y.; Nakayama, Y.; Yasuda, H. *J. Appl. Polym. Sci.* **2005**, *97*, 1008.
(19) Hagen, H.; Bezemer, C.; Boersma, J.; Kooijman, H.; Lutz, M.; Spek, A. L.; van Koten, G. *Inorg. Chem.* **2000**, *39*, 3970.
(20) Nomura, K.; Sagara, A.; Imanishi, Y. *Chem. Lett.* **2001**, 36.
(21) Nomura, K.; Sagara, A.; Imanishi, Y. *Macromolecules* **2002**, *35*, 1583.
(22) Wang, W.; Yamada, J.; Fujiki, M.; Nomura, K. *Catal. Commun.* **2003**, *4*, 159.
(23) Yamada, J.; Nomura, K. *Organometallics* **2005**, *24*, 3621.
(24) Lorber, C.; Donnadieu, B.; Choukroun, R. *J. Chem. Soc., Dalton Trans.* **2000**, 4497.
(25) Motevalli, M.; Shah, D.; Shah, S. A. A.; Sullivan, A. C. *Organometallics* **1994**, *13*, 4109.
(26) Choukroun, R.; Douziech, B.; Pan, C.; Dahan, F.; Cassoux, P. *Organometallics* **1995**, *14*, 4471.
(27) Desmangles, N.; Gambarotta, S.; Bensimon, C.; Davis, S.; Zahalka, H. *J. Organomet. Chem.* **1998**, *562*, 53.
(28) Witte, P. T.; Meetsma, A.; Hessen, B. *Organometallics* **1999**, *18*, 2944.
(29) Lorber, C.; Donnadieu, B.; Choukroun, R. *Organometallics* **2000**, *19*, 1963.
(30) Nakayama, Y.; Bando, H.; Sonobe, Y.; Suzuki, Y.; Fujita, T. *Chem. Lett.* **2003**, *32*, 766.
(31) Lorber, C.; Wolff, F.; Choukroun, R.; Vendier, L. *Eur. J. Inorg. Chem.* **2005**, 2850.

Table 1. Selected IR Data for the Compounds $V(NR)Cl_2(NHMe_2)_2$ (**1a**−**e**)

	ν(N−H) (cm^{-1})	
compd (NR group)	Nujol[a]	CH_2Cl_2[b]
1a (R = 2,6-$C_6H_3{}^iPr_2$)	3273[c]	3289
1b (R = 2-$C_6H_4{}^tBu$)	3255	3289
1c (R = 2-$C_6H_4CF_3$)	3263	3289
1d (R = ^{t}Bu)	3235	3293
1e (R = Ad)	3233	3293

[a] Nujol mull between NaCl plates. [b] CH_2Cl_2 solution, 0.1-mm-path-length NaCl cell. [c] Additional band of slightly higher intensity at 3262 cm^{-1}.

with those for **1a**. In a CH_2Cl_2 solution, the values are 3289 (arylimides) and 3293 cm^{-1} (alkylimides), but in the solid state (Nujol mull). they span a wider range (3233−3273 cm^{-1}). These observations can be interpreted as reflecting the rather different N−H···Cl hydrogen-bonded solid-state structures formed, whereas in solution, the compounds are discretely monomeric. The titanium imido compounds $Ti(NR)Cl_2(NHMe_2)_2$ in general showed analogous features.[9,32] The four new compounds **1b**−**e** gave the expected electron paramagnetic resonance (EPR) spectra as liquid or frozen solutions (discussed below).

The X-ray crystal structures of the two compounds $V(NR)Cl_2(NHMe_2)_2$ [R = 2-$C_6H_4{}^tBu$ (**1b**) or 2-$C_6H_4CF_3$ (**1c**)] have been determined. Principal bond distances and angles are compared in Table 2, and the views of the molecular structures are collected in Figure 1. Details of the structure determinations are given in the Experimental Section and Table 7 and will not be further discussed. However, it should be noted that for the purposes of discussion of the N−H···Cl bonding we refer in all instances to geometrically positioned (N−H = 0.87 Å; sp^3-hybridized nitrogen) N*H*Me_2 hydrogens.

Both compounds are monomeric and five-coordinate in the solid state (ignoring for the moment any supramolecular interactions). Crystals of **1b** exist as two different diamorphs, monoclinic and orthorhombic. The molecular structure of the monoclinic form is shown in Figure 1, and a view of the orthorhombic diamorph is given in the Supporting Information (Figure S1). While the supramolecular structures differ (see below), there are no significant differences between the two diamorphs of **1b** at the molecular level. Crystals of **1c** consist of two crystallographically independent molecules in the unit cell (again no significant differences between them), one being shown in Figure 1 and the other given in the Supporting Information (Figure S2).

The geometries at vanadium are approximately trigonal-bipyramidal ($NHMe_2$ groups axial) with N_{im}═V−Cl angles in the range 105.67(7)−112.39(6)° and N_{im}═V−N_{am} angles in the range 97.91(8)−104.48(9)°. The V═N_{im} bond lengths are 1.657(4)−1.6628(17) Å, with V═N_{im}−C angles in the range 161.10(18)−174.9(3)°, indicating a formally linear imido bond. The V−ligand distances in **1b** appear in general to be slightly longer than those for **1c**, reflecting the bulkier and more electron-releasing nature of the 2-$C_6H_4{}^tBu$ substituent compared to 2-$C_6H_4CF_3$. The structurally characterized $V(NR)Cl_2(NHMe_2)_2$ complexes described by Lorber (R = 2,6-$C_6H_3Me_2$ or 2,6-$C_6H_3{}^iPr_2$) had analogous features (e.g., V═N_{im} bond lengths of 1.654(3) and 1.656(4) Å),[33] and in general the distances and angles about the centers in **1b** and **1c** are consistent with previously reported ranges.[34,35]

Whereas Lorber's imidobis(dimethylamine) compounds showed no significant intramolecular interactions according to X-ray crystallography, the supramolecular structures of **1b** and **1c** are dominated by N−H···Cl hydrogen bonding between the $NHMe_2$ and Cl ligands of neighboring complexes. Figures 2 and 3 illustrate the extended packing in **1b** and **1c**, respectively, with each molecule donating two N−H···Cl hydrogen bonds and accepting two and each vanadium being a common member of two eight-membered rings. Broadly analogous hydrogen-bonded structures were found for $Ti(NR)Cl_2(NHMe_2)_2$ (R = ^{i}Pr, Ph, 2,3,5,6-C_6Cl_4H), while **1c** is isomorphic with $Ti(N\text{-}2\text{-}C_6H_4CF_3)Cl_2(NHMe_2)_2$.[9]

The supramolecular structure of **1c** consists of infinite N−H···Cl hydrogen-bonded bilayers (pairs of vanadium centers in the different chains are related by local noncrystallographic inversion operations) running parallel to the crystallographic *b* axis. The estimated N−H···Cl distances (average 2.72 Å; range 2.65−2.79 Å) may be categorized as "intermediate" according to the notation of Brammer, Orpen, and co-workers[36] and are somewhat less than the sum of the van der Waals radii for hydrogen and chlorine (2.95 Å[37]). The supramolecular structures of the diamorphs of **1b** differ from each other and also from that of $Ti(N\text{-}2\text{-}C_6H_4{}^tBu)Cl_2(NHMe_2)_2$. Both forms of **1b** exist as infinite N−H···Cl hydrogen-bonded chains with the same average estimated H···Cl distances (average 2.62 Å and range 2.60−2.64 Å for the two diamorphs). These are again "intermediate" in length compared to N−H···Cl hydrogen-bonded systems in general.[36] The chains for the monoclinic variant run parallel to the crystallographic *b* axis, whereas in the orthorhombic form, they run approximately parallel to the *a* axis. The two forms of **1b** differ most significantly in the relative orientations of the aryl nitrogen substituents along the chains, with those of the monoclinic form oriented in the same direction and those in the orthorhombic diamorph alternating "up" and "down". Interestingly, while both vanadium diamorphs form infinite chains, molecules of the titanium analogue $Ti(N\text{-}2\text{-}C_6H_4{}^tBu)Cl_2(NHMe_2)_2$ exist as discrete N−H···Cl hydrogen-bonded dimers in the solid state. A dimeric N−H···Cl hydrogen-bonded vanadium(4+) imido compound has been reported previously.[38]

The solid-state IR spectra (powders as Nujol mulls, Table 1) feature ν(N−H) bands at 3263 cm^{-1} for **1c** and 3255 cm^{-1}

(32) Parsons, T. B.; Hazari, N.; Cowley, A. R.; Green, J. C.; Mountford, P. *Inorg. Chem.* **2005**, 8442.
(33) Lorber, C.; Choukroun, R.; Donnadieu, B. *Inorg. Chem.* **2002**, *41*, 4217.
(34) Allen, F. H.; Kennard, O. *Chem. Des. Autom. News* **1993**, *8*, 1 and 31.
(35) Fletcher, D. A.; McMeeking, R. F.; Parkin, D. *J. Chem. Inf. Comput. Sci.* **1996**, *36*, 746 (The United Kingdom Chemical Database Service).
(36) Aullón, G.; Bellamy, D.; Brammer, L.; Bruton, E. A.; Orpen, A. G. *Chem. Commun.* **1998**, 653.
(37) Bondi, A. *J. Phys. Chem.* **1964**, *68*, 441.
(38) Pugh, S. M.; Blake, A. J.; Gade, L. H.; Mountford, P. *Inorg. Chem.* **2001**, *40*, 3992.

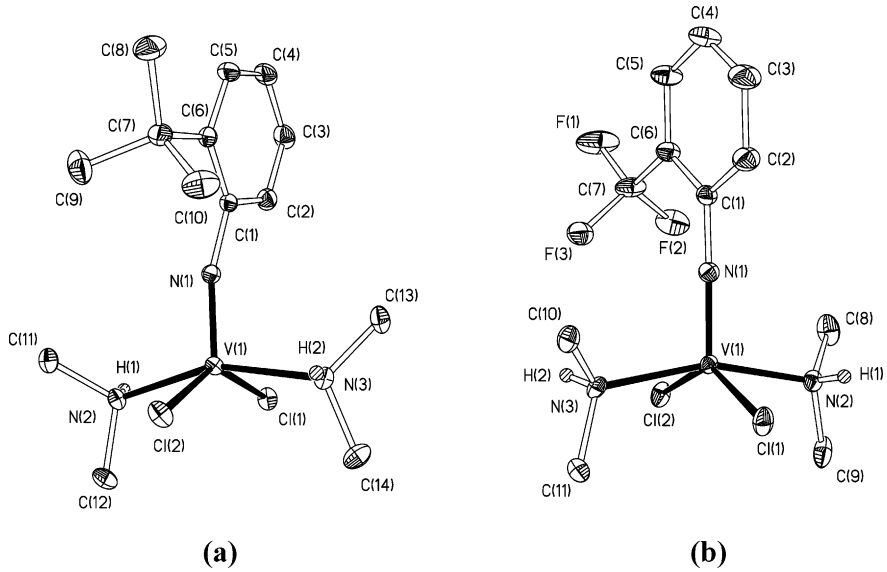

Figure 1. Displacement ellipsoid plots (25% probability) of (a) V(N-2-$C_6H_4{}^tBu$)$Cl_2(NHMe_2)_2$ (**1b**) as found in the monoclinic diamorph and (b) one of the two crystallographically independent molecules of V(N-2-$C_6H_4CF_3$)$Cl_2(NHMe_2)_2$ (**1c**). Hydrogen atoms bound to carbon are omitted and N−H atoms are drawn as spheres of the arbitrary radius. Views of **1b** found in the orthorhombic diamorph and of the other crystallographically independent molecule of **1c** are provided in the Supporting Information.

Table 2. Selected Bond Lengths (Å) and Angles (deg) for V(N-2-$C_6H_4{}^tBu$)$Cl_2(NHMe_2)_2$ (**1b**, Monoclinic and Orthorhombic Diamorphs) and V(N-2-$C_6H_4CF_3$)$Cl_2(NHMe_2)_2$ (**1c**)[a]

	1b		
	monclinic	orthorhombic	**1c**
		Lengths	
V═N_{im}	1.6584(19)	1.6628(17)	1.657(4) [1.659(4)]
V−Cl	2.3326(7)	2.3253(6)	2.3193(14) [2.3190(15)]
	2.3441(7)	2.3299(6)	2.3184(16) [2.3311(16)]
V−N_{am}	2.153(2)	2.1567(17)	2.137(5) [2.167(5)]
	2.156(2)	2.1580(17)	2.148(4) [2.149(4)]
N_{im}−C	1.404(3)	1.390(3)	1.388(5) [1.381(5)]
N_{am}H···Cl	2.64	2.63	2.67 [2.65]
	2.60	2.61	2.79 [2.75]
		Angles	
N_{im}═V−N_{am}	104.48(9)	97.91(8)	100.9(2) [101.0(2)]
	98.07(9)	98.00(8)	98.25(17) [98.48(18)]
N_{im}═V−Cl	105.67(7)	109.51(6)	108.04(13) [108.57(13)]
	110.39(8)	112.39(6)	110.53(13) [110.38(13)]
Cl−V−Cl	143.90(3)	138.09(2)	141.40(9) [141.04(10)]
N_{am}−V−N_{am}	157.45(9)	164.08(7)	160.8(2) [160.5(2)]
V═N_{im}−C	161.10(18)	163.65(15)	174.9(3) [174.1(3)]
N_{am}−H···Cl	144	142	141 [142]
	145	147	136 [138]

[a] Values in brackets for **1c** correspond to the other crystallographically independent molecule in the unit cell. Parameters involving N−H···Cl interactions are calculated assuming N−H = 0.87 Å and an sp^3-hybridized N_{am}. "N_{am}" and "N_{im}" refer to the amino ($NHMe_2$) and imido (V═NR) nitrogens, respectively.

for **1b**, consistent with the different average estimated N−H···Cl distances of 2.72 and 2.62 Å, respectively. As mentioned, the titanium compound Ti(N-2-$C_6H_4CF_3$)Cl_2-$(NHMe_2)_2$ is isomorphic with **1c**. This had an average estimated N−H···Cl distance of 2.74 Å and showed a ν(N−H) (Nujol mull) IR band at 3264 cm^{-1}. The solid-state IR spectra of the alkylimido compounds V(NR)$Cl_2(NHMe_2)_2$ [R = ^{t}Bu (**1d**) and Ad (**1e**)] showed ν(N−H) bands at 3235 and 3233 cm^{-1}, suggesting that the N−H···Cl interactions are more developed in these systems compared to **1b** and **1c**. The solid-state IR spectrum of **1a** (Table 1) featured two partially resolved ν(N−H) bands at 3273 and 3262 cm^{-1}, which at first sight suggest two N−H environments. Similar data were reported before for Ti(N-2-$C_6H_4{}^tBu$)$Cl_2(NHMe_2)_2$, the X-ray structure (vide supra) of which features one N−H···Cl hydrogen-bonded N−H group and one "free" N−H per titanium center.[9] However, the X-ray structure of **1a** reported by Lorber appears to show no significant N−H···Cl contacts, and the IR data (Nujol) reported previously for **1a** are identical within error to those in Table 1 recorded by us. One explanation could be that the sample used for the X-ray structure was of a rather different solid-state form than that obtained from the reaction mixture.

Synthesis and Characterization of the Precatalyst Families V(NR)(*fac*-N_3)Cl_2 [*fac*-N_3 = TACN (2) or TPM (3)]. The reaction between a benzene solution of **1a** and TACN heated to 80 °C resulted in the precipitation and subsequent isolation of the target compound V(N-2,6-$C_6H_3{}^iPr_2$)(TACN)Cl_2 (**2a**) in 73% yield. This general protocol was extended to afford the compounds V(NR)(TACN)Cl_2 (**2b**−**e**) and V(NR)(TPM)Cl_2 (**3a**−**e**) as red or green air- and moisture-sensitive solids in 39−73% isolated yields (Scheme 1). Full details of the characterizing data are provided in the Experimental Section, and detailed experimental procedures are provided in the Supporting Information. Compounds **2** and **3** are the first vanadium imido complexes of TACN or TPM. The isoelectronic oxo complex V(O)(TACN)Cl_2 has been reported previously.[39] Vanadium TACN complexes in general are well-known, whereas vanadium TPM complexes are very rare.[40] The vanadium(2+) sandwich cation $[V\{HC(pz)_3\}_2]^{2+}$ has been described,[41] and a series of VFe_3S_4 clusters [formally containing vanadium(3+)] capped with tris(pyrazolyl)methanesulfonate ligands have also been prepared, namely, $[\{O_3SC(pz)_3\}VFe_3S_4X_3]^{2-}$ (X = Cl, SEt, S-4-

(39) Fiedler, D.; Miljanic, O. S.; Welch, E. J. *Acta Crystallogr., Sect. E* **2002**, *58*, m347.
(40) Bigmore, H. R.; Lawrence, S. C.; Mountford, P.; Tredget, C. S. *Dalton Trans.* **2005**, 635 (Perspective Article review).
(41) Mani, F. *Inorg. Chim. Acta* **1980**, *38*, 97.

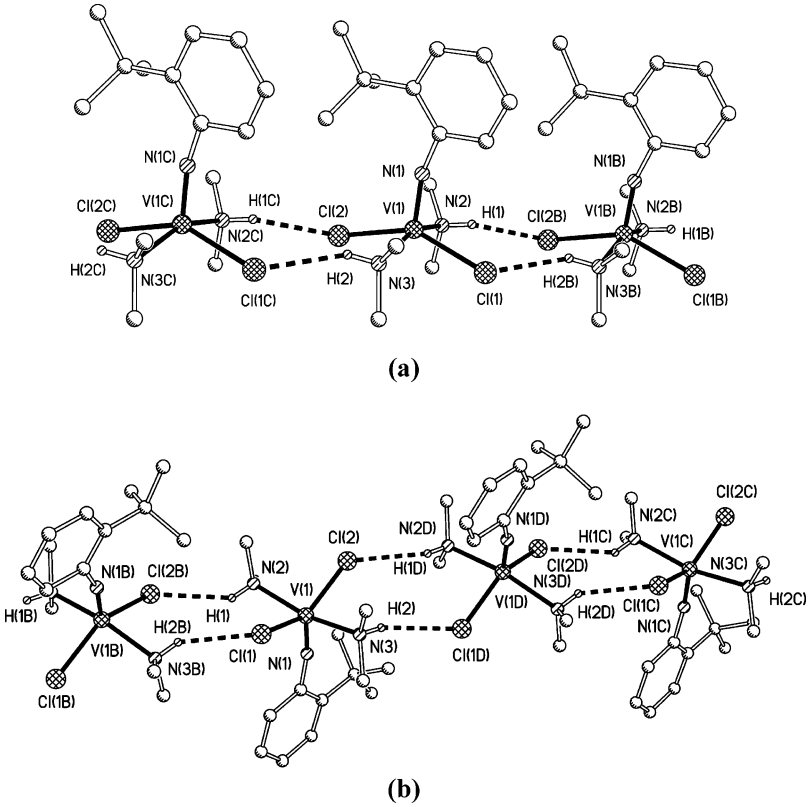

Figure 2. Extended interaction diagrams for V(N-2-$C_6H_4{}^tBu$)$Cl_2(NHMe_2)_2$ (**1b**) showing a portion of the infinite N−H···Cl hydrogen-bonded chains. Hydrogen atoms bound to carbon are omitted, and all atoms are drawn as spheres of the arbitrary radius. (a) Monoclinic form, symmetry operators: B, x, $y + 1$, z; C, x, $y - 1$, z. (b) Orthorhombic form, symmetry operators: B, $x + {}^1/_2$, y, $-z + {}^1/_2$; C, $x - 1$, y, z; D $x - {}^1/_2$, y, $-z + {}^1/_2$.

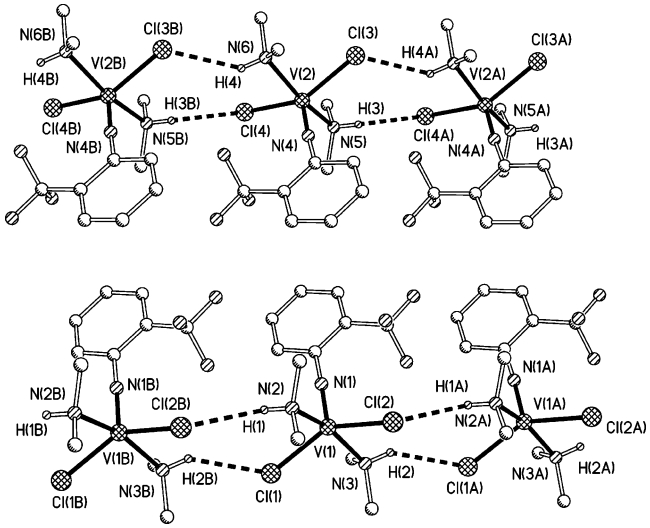

Figure 3. Extended interaction diagram for V(N-2-$C_6H_4CF_3$)$Cl_2(NHMe_2)_2$ (**1c**) showing a portion of the infinite N−H···Cl hydrogen-bonded bilayers. Hydrogen atoms bound to carbon are omitted, and all atoms are drawn as spheres of the arbitrary radius. Symmetry operators: A, x, $y + 1$, z; B, x, $y - 1$, z.

C_6H_4Me, O-4-C_6H_4Me).[42] Tris(pyrazolyl)*borate*-supported vanadium(5+) imido compounds are somewhat better established, as mentioned above, and three have been structurally characterized.[14,43]

Scheme 1. Synthesis of V(NR)(TACN)Cl_2 (**2a**−**e**) and V(NR)(TPM)Cl_2 (**3a**−**e**)

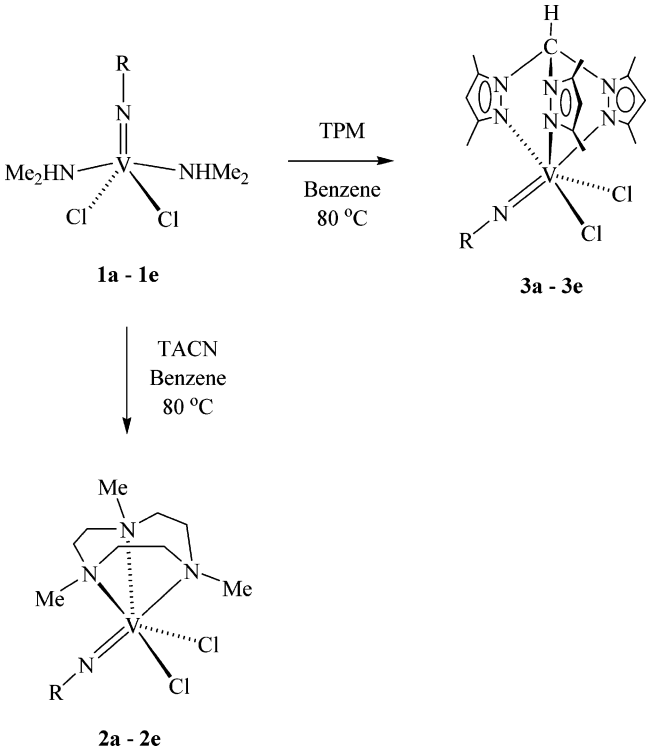

The X-ray crystal structures for the TACN compounds V(NR)(TACN)Cl_2 [R = 2-$C_6H_4{}^tBu$ (**2b**), 2-$C_6H_4CF_3$ (**2c**), or ^tBu (**2d**)] have been determined. Selected bond distances and angles are presented in Table 3, and views of the

(42) Fomitchev, D. V.; McLauchlan, C. C.; Holm, R. H. *Inorg. Chem.* **2002**, *41*, 958.
(43) Oshiki, T.; Mashima, K.; Kawamura, S.; Tani, K.; Kitaura, K. *Bull. Chem. Soc. Jpn.* **2000**, *73*, 1735.

Table 3. Selected Bond Lengths (Å) and Angles (deg) for V(NR)(TACN)Cl_2 [R = 2-C_6H_4^{t}Bu (**2b**), 2-$C_6H_4CF_3$ (**2c**), or ^{t}Bu (**2d**)]

	2b	**2c**	**2d**
	Lengths		
V(1)−N(1)	2.354(2)	2.3379(17)	2.340(8)
V(1)−N(2)	2.204(2)	2.2063(17)	2.209(8)
V(1)−N(3)	2.215(2)	2.2011(16)	2.218(8)
V(1)−N(4)	1.704(2)	1.6925(17)	1.657(2)
V(1)−Cl(1)	2.3845(7)	2.3766(6)	2.4030(7)
V(1)−Cl(2)	2.3872(2)	2.3801(6)	2.4011(7)
	Angles		
Cl(1)−V(1)−Cl(2)	93.33(2)	92.65(2)	92.67(3)
Cl(1)−V(1)−N(1)	86.72(6)	86.21(4)	89.76(15)
Cl(1)−V(1)−N(2)	162.23(6)	162.98(5)	91.44(18)
Cl(1)−V(1)−N(3)	90.64(6)	93.91(5)	165.35(16)
Cl(1)−V(1)−N(4)	99.83(7)	93.07(6)	97.54(7)
Cl(2)−V(1)−N(1)	84.82(5)	89.43(5)	88.33(15)
Cl(2)−V(1)−N(2)	90.82(6)	89.75(5)	165.03(19)
Cl(2)−V(1)−N(3)	161.19(6)	164.46(5)	92.81(16)
Cl(2)−V(1)−N(4)	94.71(7)	100.60(6)	96.72(7)
N(1)−V(1)−N(2)	76.45(8)	76.97(6)	77.3(2)
N(1)−V(1)−N(3)	77.05(7)	76.98(6)	76.8(2)
N(1)−V(1)−N(4)	173.45(8)	169.97(7)	170.89(16)
N(2)−V(1)−N(3)	80.18(8)	79.97(7)	80.0(2)
N(2)−V(1)−N(4)	97.04(9)	103.05(7)	96.99(19)
N(3)−V(1)−N(4)	102.72(8)	93.10(7)	95.30(16)
V(1)−N(4)−C(10)	158.92(17)	159.21(15)	170.20(18)

molecular structures are collected in Figure 4. All three compounds exist as monomeric, six-coordinate complexes in the solid state. In each case, the TACN ligand is κ^3-coordinated, with the remainder of the coordination sphere occupied by the imido ligand and two *cis*-chloride ligands. Minor disorder in the TACN rings of all three was satisfactorily resolved. Compound **2d** is isomorphic with Ti(N^{t}Bu)(TACN)Cl_2 (both obtained as CH_2Cl_2 solvates).

A comparison of the V(1)−N(4) distances in the three structures shows that the *tert*-butylimido ligand in **2d** has the shortest V═N_{im} bond [1.657(2) Å compared with 1.704(2) and 1.6925(17) Å]. The longest V−Cl distances are also found for **2d**, highlighting the electron-releasing properties of the alkylimido group in comparison to the arylimido groups, as is generally observed. The V═N_{im} bond lengths lie within the previously reported range for vanadium(4+) imido compounds (1.623−1.730 Å, average 1.679 Å, for 18 entries in the Cambridge Structural Database[34,35]). The V═N_{im}−C bond angles fall in the range 158.92(17)−170.20(18)°, indicating formally linear imido linkages and that the imido groups are acting as four-electron donors. The comparatively low V═N_{im}−C_{ipso} angles for **2b** [158.92(17)°] and **2c** [159.21(15)°] are attributed to steric repulsions between the bulky ortho substituents and the other ligands present. The V−N bond lengths trans to the imido ligands are significantly longer than the other two V−N bonds [V(1)−N(1) = 2.3379(17)−2.354(2) Å compared with V(1)−N(2) = 2.204(2)−2.209(8) Å and V(1)−N(3) = 2.215(2)−2.2011(16) Å] due to the strong trans influence of imido ligands. This is consistent with the structures of the titanium(4+) complexes Ti(NR)(TACN)Cl_2[10] and with that of the V−N bond length trans to the oxo ligand in V(O)(TACN)Cl_2.[39] A number of vanadium TACN complexes have been structurally characterized previously (26 entries in the Cambridge Structural Database[34,35]).

The X-ray crystal structures for the TPM compounds V(NR)(TPM)Cl_2 [R = 2,6-$C_6H_3^{i}Pr_2$ (**3a**), 2-C_6H_4^{t}Bu (**3b**), 2-$C_6H_4CF_3$ (**3c**), or Ad (**3e**)] have also been determined. Selected bond distances and angles are compared in Table 4, and views of the molecular structures are given in Figure 5. As for the TACN homologues, all four compounds exist as monomeric, six-coordinate complexes in the solid state. The tridentate TPM ligand is facially coordinating through three of the six pyrazolyl ring nitrogens. The remainder of the coordination sphere is again completed by the imido and two chloride ligands. The V═N_{im}−C bond angles fall in the range 157.48(16)−172.8(3)° and so may also be considered linear. A comparison of the V═N_{im}−C bond angles for the three arylimido groups (**3a**−**c**) shows that the more bulky ortho groups in **3b** and **3c** have led to slightly more bent V═N_{im}−C linkages compared to that found in **3a** [162.9(3) and 157.48(16)° vs 172.8(3)°, respectively). This apparent steric effect is highlighted further when considering the adamantylimido ligand in **3e**, which has an associated V═N_{im}−C angle of 158.7(4)° [159.4(4)° for the second orientation of the disordered Ad group]. The imido nitrogen substituent bends "down" away from the TPM ligand in **3c** and **3e**, whereas for **3b**, the aryl group bends "up" toward the TPM, presumably reflecting the repulsion between the *o*-*tert*-butyl group and the chloride ligands.

As in the V(NR)(TACN)Cl_2 complexes, there is significant lengthening of the V−N bond trans to the imido ligand [V(1)−N(1) = 2.262(3)−2.328(3) Å compared with V(1)−N(3) = 2.1500(17)−2.170(3) Å and V(1)−N(5) = 2.1513(17)−2.170(3) Å]. As was also found in the V(NR)(TACN)Cl_2 systems, the alkylimido ligand leads to a shorter V═N_{im} bond length compared to the arylimides [1.663(3) Å (**3e**) compared to 1.677(3)−1.686(3) Å]. In general, the V−N_{TACN} distances in the compounds **2** are longer than those in comparable TPM-supported complexes **3** (for example, the average V−N_{TACN} distance in **2b** is 2.258 Å, whereas that in **3b** is 2.200 Å). A similar feature was noted recently for the titanium(4+) complexes Ti(N^{t}Bu)(TACN)Cl_2 (average Ti−N_{TACN} = 2.377 Å)[10] and Ti(N^{t}Bu)(TPM)Cl_2 (average Ti−N_{TPM} = 2.291 Å)[44] and also the compounds Sc(TACN)$(CH_2SiMe_3)_3$ (average Sc−N_{TACN} = 2.463 Å) and Sc(TPM)$(CH_2SiMe_3)_3$ (average Sc−N_{TPM} = 2.420 Å).[45]

The compound **3a** is isomorphic with Kress's tris(pyrazolyl)borate vanadium(5+) compound V(N-2,6-$C_6H_3^{i}Pr_2$)(Tp*)Cl_2 [Tp* = HB(Me_2pz)$_3$].[14] The V−Cl (average 2.298 Å) and V−N_{Tp*} (average 2.147 Å) distances in the Tp* compound are shorter, as expected, than those in **3a** (average V−Cl = 2.389 Å; average V−N_{TPM} = 2.217 Å) because the former contains vanadium(5+) and the *fac*-N_3 ligand carries a formal negative charge. Surprisingly, however, the V═N_{im} distance in **3a** of 1.677(3) Å is shorter than that in the Tp* homologue [V═N_{im} = 1.693(4) Å]. Analogous features were seen in the related compound V(N-2,6-C_6H_3-

(44) Lawrence, S. C. D. Phil. Thesis, University of Oxford, Oxford, U.K., 2003.
(45) Tredget, C. S.; Lawrence, S. C.; Ward, B. D.; Howe, R. G.; Cowley, A. R.; Mountford, P. *Organometallics* **2005**, *24*, 3136.

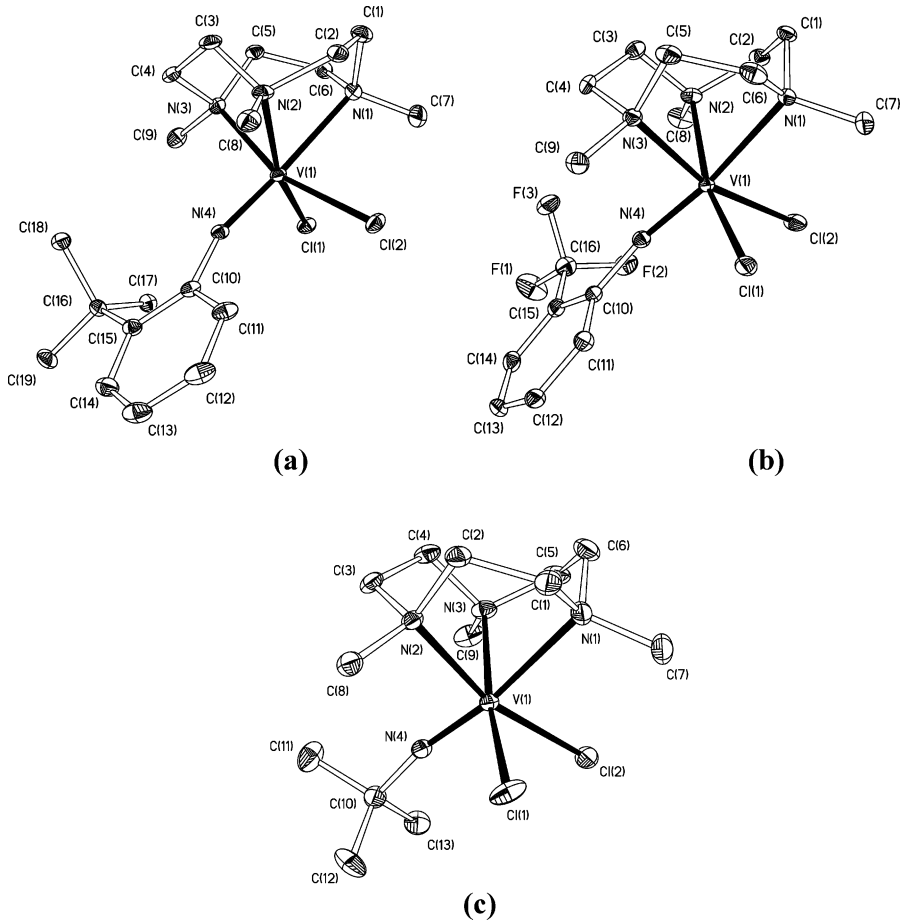

Figure 4. Displacement ellipsoid plots (25% probability) of (a) V(N-2-$C_6H_4{}^tBu$)(TACN)Cl_2 (**2b**), (b) V(N-2-$C_6H_4CF_3$)(TACN)Cl_2 (**2c**), and (c) V(N^tBu)(TACN)Cl_2 (**2d**). Hydrogen atoms and CH_2Cl_2 of crystallization (for **2d**) are omitted. The minor orientations of the disordered TACN ligands are also not shown.

Table 4. Selected Bond Lengths (Å) and Angles (deg) for V(NR)(TPM)Cl_2 [R = 2,6-$C_6H_3{}^iPr_2$ (**3a**), 2-$C_6H_4{}^tBu$ (**3b**), 2-$C_6H_4CF_3$ (**3c**), or Ad (**3e**, Values for the Other Orientation of the NAd Group Given in the Supporting Information)][a]

	3a	3b	3c	3e
		Lengths		
V(1)−N(1)	2.328(3)	2.272(3) [2.262(3)]	2.3186(17)	2.302(2)
V(1)−N(3)	2.155(3)	2.170(3) [2.166(3)]	2.1500(17)	2.179(2)
V(1)−N(5)	2.169(3)	2.170(3) [2.160(3)]	2.1513(17)	2.175(2)
V(1)−N(7)	1.677(3)	1.684(3) [1.686(3)]	1.6795(17)	1.663(3)
V(1)−Cl(1)	2.3860(10)	2.3832(10) [2.3702(11)]	2.3675(6)	2.4024(9)
V(1)−Cl(2)	2.3920(10)	2.3893(10) [2.3932(11)]	2.3686(6)	2.4137(8)
		Angles		
Cl(1)−V(1)−Cl(2)	93.48(4)	94.74(4) [94.69(4)]	92.50(2)	96.16(3)
Cl(1)−V(1)−N(1)	86.31(8)	87.73(8) [86.64(8)]	86.19(4)	83.98(6)
Cl(1)−V(1)−N(3)	164.48(8)	166.72(9) [165.84(9)]	165.18(5)	163.08(7)
Cl(1)−V(1)−N(5)	90.48(8)	90.14(8) [89.82(9)]	89.53(5)	89.08(7)
Cl(1)−V(1)−N(7)	99.33(11)	99.65(11) [100.68(11)]	93.96(6)	94.45(11)
Cl(2)−V(1)−N(1)	86.82(8)	85.57(8) [85.86(8)]	87.67(4)	83.52(6)
Cl(2)−V(1)−N(3)	86.19(8)	89.01(8) [89.49(9)]	91.46(5)	89.49(7)
Cl(2)−V(1)−N(5)	164.97(8)	164.26(9) [165.07(9)]	166.87(5)	162.27(7)
Cl(2)−V(1)−N(7)	100.71(11)	101.12(11) [101.09(11)]	96.16(6)	95.02(10)
N(1)−V(1)−N(3)	78.56(11)	79.85(11) [80.16(11)]	79.71(6)	80.82(9)
N(1)−V(1)−N(5)	78.96(11)	79.67(11) [80.20(11)]	79.52(6)	80.19(9)
N(1)−V(1)−N(7)	170.23(13)	169.50(13) [169.36(13)]	176.15(7)	177.72(10)
N(3)−V(1)−N(5)	83.27(11)	83.07(11) [82.93(12)]	83.48(6)	81.08(9)
N(3)−V(1)−N(7)	95.18(13)	92.09(13) [91.76(13)]	99.80(8)	100.95(12)
N(5)−V(1)−N(7)	92.94(13)	92.77(13) [92.01(14)]	96.64(7)	101.47(12)
V(1)−N(7)−C(17)	172.8(3)	162.9(3) [162.9(3)]	157.48(16)	158.7(4)

[a] Values in brackets for **3b** correspond to the other crystallographically independent molecule in the unit cell.

Me_2)(Tp*)Cl_2 [V═N_{im} = 1.687(3) Å; average V−Cl = 2.296 Å; V−N_{Tp*} = 2.153 Å].[43] We speculate that the tighter binding of the Tp* and chlorine ligands in the vanadium-(5+) complexes leads to a destabilizing effect on the V═NAr moiety, but further work would be needed to confirm this.

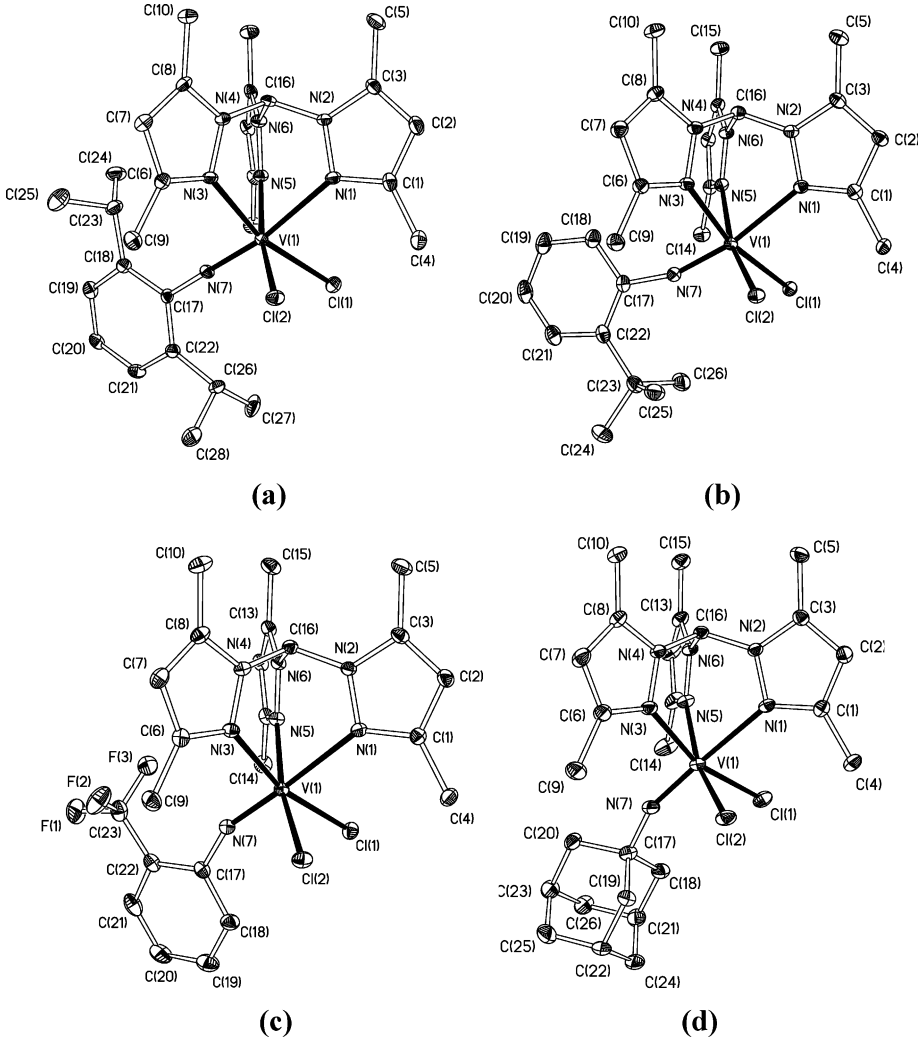

Figure 5. Displacement ellipsoid plots (25% probability) of (a) V(N-2,6-$C_6H_3{}^iPr_2$)(TPM)Cl_2 (**3a**), (b) V(N-2-$C_6H_4{}^tBu$)(TPM)Cl_2 (**3b**), (c) V(N-2-C_6H_4-CF_3)(TPM)Cl_2 (**3c**), and (d) V(NAd)(TPM)Cl_2 (**3e**, one orientation of the disordered Ad group shown). Hydrogen atoms and CH_2Cl_2 of crystallization (for **3b**, **3c**, and **3e**) are omitted. A view of the other crystallographically independent molecule of **3b** are provided in the Supporting Information.

It is interesting to compare the orientations of the imido *N*-aryl group in the compounds V(N-2-C_6H_4R)(TACN)Cl_2 [R = ^{t}Bu (**2b**) or CF_3 (**2c**)], V(N-2-C_6H_4R)(TPM)Cl_2 [R = ^{t}Bu (**3b**) or CF_3 (**3c**)], and the corresponding structurally characterized titanium analogues Ti(N-2-C_6H_4R)(TPM)-Cl_2.[11,46] In the TACN compounds **2b** and **2c**, the bulky ortho substituent is oriented to one side of the VCl_2 moiety, whereas in **3b** and also both Ti compounds Ti(N-2-C_6H_4R)-(TPM)Cl_2 (R = ^{t}Bu or CF_3), the ortho groups are projected down, i.e., directly away from the TPM ligand, and lie under the VCl_2 or $TiCl_2$ moieties. This allows the C_6 ring carbons to lie within the cleft formed by the two Me_2pz rings [those containing N(3), N(4) and N(5), N(6) in Figure 5b]. The same orientating effect is seen in **3a** and **3c** [and also V(N-2,6-$C_6H_3R_2$)(Tp*)Cl_2 (R = Me, ^{i}Pr)[14,43]], with the aryl ring lying in the plane that bisects the Cl−V−Cl angle.

Unusually, at least based on the structures of **3b** and Ti-(N-2-C_6H_4R)(TPM)Cl_2 (R = ^{t}Bu or CF_3) the *o*-CF_3 substituent in **3c** is not oriented away from the TPM ligand but instead lies in the cleft between two Me_2pz rings. This orientation may be chosen to best minimize the repulsions between the *o*-CF_3 substituent and the chloride ligands at the shorter metal−ligand bond distances in **3c**. The shortest F···H distance is 2.36 Å [associated angle F(2)···H(93)−C(9) = 144 °; C−H bond orientations determined from a Fourier difference map and hydrogen atoms placed with an ideal C−H = 1.08 Å]. This is less than the sum of the van der Waals radii for fluorine and hydrogen (2.5−2.7 Å) but lies at the long end of the range of F···H distances considered to be significant (F···H hydrogen-bond interactions are in general deemed to be very weak).[47,48]

EPR Studies. The EPR spectra of V(NR)Cl_2($NHMe_2$)$_2$ (**1b**−**e**), **2a**−**e**, and **3a**−**e** in a CH_2Cl_2/toluene (ca. 9:1, v/v) solution were recorded at 295 and 120 K. Details of the spectral features are summarized in Table 5. The EPR parameters listed were extracted from spectral simulations. All frozen solution spectra show hyperfine structure typical of vanadium(4+) (^{51}V, $I = {}^7/_2$, 100% natural abundance) with anisotropy of the **g** matrices (*g* factor) and **A** matrices

(46) Sealey, A. J. D. Phil. Thesis, University of Oxford, Oxford, U.K., 2004.

(47) Howard, J. A. K.; Hoy, V. J.; O'Hagan, D.; Smith, G. T. *Tetrahedron* **1996**, *52*, 12613.

(48) Dunitz, J. D.; Taylor, R. *Chem.*−*Eur. J.* **1997**, *3*, 89.

Table 5. EPR Data for $V(NR)Cl_2(NHMe_2)_2$ (**1**), $V(NR)(TACN)Cl_2$ (**2**), and $V(NR)(TPM)Cl_2$ (**3**) in a CH_2Cl_2/Toluene (ca. 9:1, v/v) Solution [R = 2,6-$C_6H_3{}^iPr_2$ (**a**), 2-$C_6H_4{}^tBu$ (**b**), 2-$C_6H_4CF_3$ (**c**), ^{t}Bu (**d**), or Ad (**e**)][a]

	292 K solution		120 K frozen solution						
compd	g_{iso}	A_{iso}	g_{xx}	g_{yy}	g_{zz}	g_{iso}	A_{xx}	A_{yy}	A_{zz}
1b	1.973	94	1.986	1.985	1.948	1.973	56	58	168
1c	1.971	93	1.986	1.985	1.947	1.973	55	56	167
1d	1.973	101	1.988	1.986	1.945	1.973	58	59	172
1e	1.975	97	1.988	1.987	1.945	1.973	58	59	172
2a	1.972	95	1.986	1.979	1.947	1.971	60	58	167
2b	1.969	93	1.990	1.977	1.946	1.971	59	56	166
2c	1.972	94	1.983	1.976	1.952	1.970	61	61	167
2d	1.973	97	1.989	1.983	1.946	1.973	61	59	171
2e	1.975	97	1.990	1.983	1.945	1.973	62	59	171
3a	1.973	96	1.987	1.979	1.944	1.970	62	62	169
3b	1.973	98	1.987	1.981	1.945	1.971	63	63	170
3c	1.974	95	1.987	1.979	1.949	1.972	61	62	168
3d	1.972	100	1.989	1.981	1.940	1.970	64	65	174
3e	1.973	100	1.990	1.984	1.942	1.972	64	65	174

[a] Experimental errors $\Delta g_{ii} = \pm 0.001$ and $\Delta A_{ii} = \pm 2$.

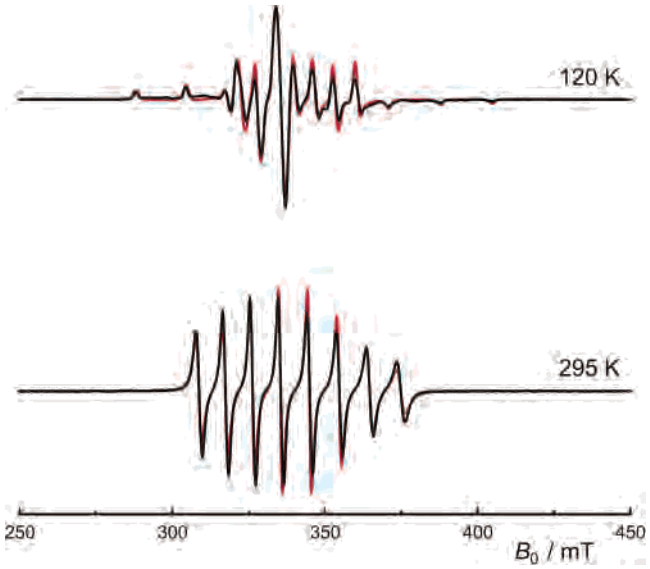

Figure 6. EPR spectra (black lines) of V(N-2,6-$C_6H_3{}^iPr_2$)(TACN)Cl_2 (**2a**) [top, frozen solution (120 K); bottom, solution at 295 K] and their simulations (red lines). The solvent is a CH_2Cl_2/toluene (ca. 9:1, v/v) mixture. Spectra were recorded at 9.450-GHz (X-band) frequency with a microwave power of 2 mW and a modulation amplitude of 0.5 mT.

(hyperfine splitting). The 295 K spectra comprise eight hyperfine lines characteristic of the interaction of the unpaired (vanadium-centered) electron with the ^{51}V nucleus. By way of example, the frozen- and liquid-solution EPR spectra of **2a** are shown in Figure 6.

The frozen-solution spectra are rhombic, consistent with the molecular symmetries in each case and consistent with retention of the solid-state structures in solution. The local crystal fields are dominated by the imido ligands (defining the local *z* axes). The *g* and *A* values are consistent with vanadium(4+) imido compounds in general.[33,38,49] The A_{iso} and A_{zz} values for the arylimido compounds (**1**−**3**, suffixes **a**−**c**) are slightly but persistently smaller than those for the alkylimides (suffixes **d** and **e**), suggesting a slightly greater degree of covalency (or 3d electron delocalization) in the arylimido systems. The effect is rather small, however, and may be because the 3d orbital containing the unpaired electron (in the local *xy* plane of **1**−**3**, *z* axis defined as above) lies orthogonal to the principal $3d_\pi-2p_\pi$ bonding orbitals (involving $3d_{xz}$ and $3d_{yz}$ in the same coordinate system). This is also consistent with the lack of hyperfine coupling to the imido nitrogen.

Ethylene Polymerization Studies. Representative examples of the three vanadium(4+) imido familes $V(NR)Cl_2(NHMe_2)_2$ (**1**), $V(NR)(TACN)Cl_2$ (**2**), and $V(NR)(TPM)Cl_2$ (**3**) were screened for ethylene polymerization using MAO cocatalyst (Al:V = 1500:1) initiated at 22−24 °C, these being conditions identical with those used for room-temperature screening of the corresponding TACN- and TPM-supported titanium imido precatalysts $Ti(NR)(fac\text{-}N_3)Cl_2$.[10,11] Disappointingly, none of the TACN catalysts assessed (**2a**−**d**) showed any polymerization activity under these conditions, whereas the titanium analogues gave productivities of up to 760 kg mol^{-1} h^{-1} bar^{-1} (R = ^{t}Bu). The polymerization results for catalysts of the types **1** and **3** are summarized in Table 6. Assessment of **3b** with MAO activation at 55 °C showed a productivity of 28 kg mol^{-1} h^{-1} bar^{-1} comparable to that obtained at the lower temperature (30 kg mol^{-1} h^{-1} bar^{-1}). None of the systems showed any significant productivity when activated with Et_2AlCl (Al:V = 1000:1).

The imidobis(dimethylamine) precatalysts **1a**, **1b**, and **1d** (entries 1−3, Table 6) gave modest productivities of 9−16 kg mol^{-1} h^{-1} bar^{-1}, each forming high-M_w polyethylene (PE) with fairly broad M_w/M_n values in the range of 4.5−6.0. The ethylene uptake traces were all rather similar (Figure S7 of the Supporting Information) and showed a very sluggish uptake over the 30 min of the polymerization run. The productivity of 16 kg mol^{-1} h^{-1} bar^{-1} for **1a** is comparable to the figure reported by Lorber (59 kg mol^{-1} h^{-1} bar^{-1} for a 10-min run time). From the polymer yield and M_n, it can be estimated that no more than ca. 15% of the vanadium centers in catalysts **1** are productive and may be considerably fewer.

The TPM-supported catalysts $V(NR)(TPM)Cl_2$ (**3a**−**d**) also showed generally low productivities in the range 6−30 kg mol^{-1} h^{-1} bar^{-1} (entries 4−7, Table 6). However, unlike the results for the imido−diamine systems **1**, the TPM-supported catalysts showed ethylene uptakes (Figure 7) and PE molecular weight distributions (Figure 8), which varied significantly with the imido R substituent. The observation that the arylimides **3a**−**c** had productivities some 3−5 times that of **3d** mirrors the situation for the MAO-activated titanium imido systems $Ti(NR)(TPM)Cl_2$ (R = ^{t}Bu, 230 kg mol^{-1} h^{-1} bar^{-1}; R = 2-$C_6H_4{}^tBu$, 2-$C_6H_4CF_3$, or 2,6-$C_6H_3{}^iPr_2$, 810−1170 kg mol^{-1} h^{-1} bar^{-1}). However, while the overall trend in the relative productivity as a function of the imido nitrogen substituent is similar for the vanadium(4+) and titanium(4+) systems, the latter are clearly much more productive under very similar conditions.

The *tert*-butylimido catalyst system **3d**/MAO showed little or no ethylene uptake after the first ca. 5 min (on average, only about 0.1 PE chains per precatalyst metal center was

(49) Lorber, C.; Choukroun, R.; Donnadieu, B. *Inorg. Chem.* **2003**, *42*, 673.

Table 6. Ethylene Polymerization Data for Imido Vanadium Catalysts[a]

entry	precatalyst	yield of PE (g)	productivity (kg mol^{-1} h^{-1} bar^{-1})	M_w (g mol^{-1})	M_n (g mol^{-1})	M_w/M_n
1	V(N-2,6-$C_6H_3{}^iPr_2$)Cl_2(NHMe$_2$)$_2$ (**1a**)	0.25	16	1 355 000	298 500	4.5
2	V(N-2-$C_6H_4{}^tBu$)Cl_2(NHMe$_2$)$_2$ (**1b**)	0.14	9	1 535 000	299 000	5.1
3	V(N^{t}Bu)Cl_2(NHMe$_2$)$_2$ (**1d**)	0.15	10	1 545 000	258 000	6.0
4	V(N-2,6-$C_6H_3{}^iPr_2$)(TPM)Cl_2 (**3a**)	0.29	19	165 500	2 730	61
5	V(N-2-$C_6H_4{}^tBu$)(TPM)Cl_2 (**3b**)	0.45	30	*b*	*b*	*b*
6	V(N-2-$C_6H_4CF_3$)(TPM)Cl_2 (**3c**)	0.29	19	*c*	*c*	*c*
7	V(N^{t}Bu)(TPM)Cl_2 (**3d**)	0.09	6	755 500	138 500	5.5

[a] Conditions: 6 bar C_2H_4, 5 μmol of precatalyst, MAO, Al:V = 1500:1, 250 mL of toluene, 30 min, initiation temperature = 22−24 °C; yields are the average of two runs in each case. [b] Bimodal polymer. High-M_w fraction (18 wt %): M_n = 240 500, M_w = 1 270 000, M_w/M_n = 5.3. Low-M_w fraction (82 wt %): M_n = 670, M_w = 840, M_w/M_n = 1.3. [c] Bimodal polymer. High-M_w fraction (58 wt %): M_n = 187 000, M_w = 1 145 000, M_w/M_n = 6.1. Low-M_w fraction (42 wt %): M_n = 745, M_w = 1085, M_w/M_n = 1.5.

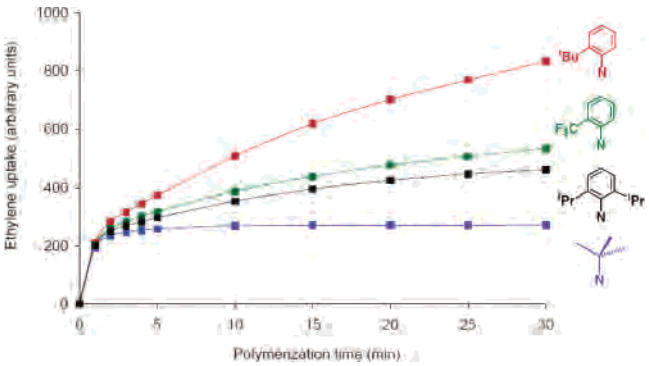

Figure 7. Ethylene uptake by the V(NR)(TPM)Cl_2 [R = 2,6-$C_6H_3{}^iPr_2$ (**3a**), 2-$C_6H_4{}^tBu$ (**3b**), 2-$C_6H_4CF_3$ (**3c**), ^{t}Bu (**3d**)]/MAO catalyst systems.

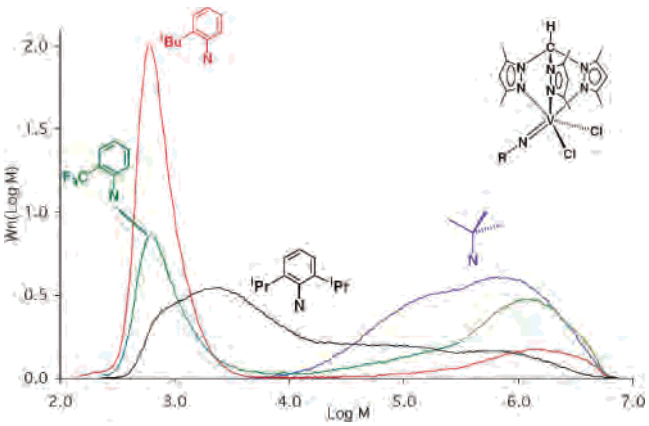

Figure 8. Molecular weight distributions determined by GPC for the PEs produced by V(NR)(TPM)Cl_2 [R = 2,6-$C_6H_3{}^iPr_2$ (**3a**), 2-$C_6H_4{}^tBu$ (**3b**), 2-$C_6H_4CF_3$ (**3c**), ^{t}Bu (**3d**)].

produced), whereas all three arylimides **3a**−**c** maintained some productivity over the full 30 min run time, with the bulkier precatalyst **3b** being superior (Figure 7). The PE formed with **3a**/MAO has a very broad molecular weight distribution indeed (Figure 8), whereas that formed with **3b**/MAO is effectively bimodal. The PE formed with **3c**/MAO had features reminiscent of that from **3b**/MAO but with a more dominant high-M_w part. The PE produced with **3d**/MAO was of quite high M_w and had a broad molecular weight distribution. The very low M_w fraction (ca. 80 wt % of the total) of the PE formed with **3b** has a narrow M_w/M_n value of 1.3, while the high-M_w fraction has a broader M_w/M_n of 5.3. The low-M_w part may be estimated to represent 110 chains per total metal present and the high-M_w part only ca. 0.1 chains per metal center. The low-M_w fraction was sufficiently soluble in hot (100 °C) 1,2-$C_6D_4Cl_2$ to allow analysis by ^{1}H NMR spectroscopy. End-group analysis and integration found a M_n of ca. 800 [cf. 670 by gel permeation chromatography (GPC; Table 6)] and that ca. 35% of the chains were terminated by vinyl groups. Therefore, under these conditions and polymerization run time, chain transfer to monomer is significant but transfer to aluminum is dominant.

The M_w and molecular weight distributions for PE produced by the vanadium(4+) TPM-supported catalyst systems differ significantly from those for the titanium(4+) analogues Ti(NR)(TPM)Cl_2.[11] In particular, the titanium analogues of **3b** (R = 2-$C_6H_4{}^tBu$) and **3c** (R = $C_6H_4CF_3$) gave PE with M_w = 843 000 and 1 107 000 and M_w/M_n values of 7.0 and 3.6, respectively, under comparable conditions. Unfortunately, the PE formed by the titanium analogue of **3b** under the same polymerization conditions was too insoluble for analysis by NMR spectroscopy, and so an exact comparison with **3b**/MAO cannot be made.[46]

The lower (or lack of) activity of vanadium-based Ziegler−Natta catalysts in general compared to their titanium or other group 4 analogues is well-known and attributed in general to deactivation via reduction pathways.[12,13] Gibson has explicitly demonstrated that cyclopentadienyl-supported vanadium(5+) imido catalysts probably deactivate via reductive bimolecular pathways.[16,50] The superior productivity of the bulkier imido catalyst **3b** may be connected with these observations.

The poor behavior of the vanadium(4+) catalysts V(NR)(*fac*-N_3)Cl_2 (**2** and **3**) in comparison with the corresponding (and highly productive) isostructural titanium(4+) systems is also consistent with previous reports. Choukroun et al. found that [Cp_2VMe]$^+$ is unreactive toward ethylene polymerization[26] in contrast to the titanocenium analogues.[51] It was also reported that a diamide-supported vanadium(4+) catalyst (MAO activation) had a productivity that was only ca. 10% of that of the titanium analogue.[29] Hessen and coworkers have shown that the MAO-activated vanadium(4+) constrained geometry catalyst (CGC) V(η,$^5\eta^1$-$C_5H_4CH_2$-CH_2N^iPr)Cl_2 had a productivity that was ca. 40% of the corresponding titanium(4+) system; moreover, the PE formed

(50) Chan, M. C. W.; Cole, J. M.; Gibson, V. C.; Howard, J. K. *Chem. Commun.* **1997**, 2345.
(51) Bochmann, M. *J. Chem. Soc., Dalton Trans.* **1996**, 255.

with the vanadium catalyst had a M_w that was significantly lower [M_n = 4900 for vanadium(4+) vs 59 500 for titanium(4+)].[28]

Conclusions

We have found that bulky alkyl- and arylimido−diamine complexes V(NR)Cl_2(NHMe_2)$_2$ (**1**) may be accessed via the straightforward route first described by Lorber only for less sterically demanding aryl substituents. However, unlike the previous arylimido homologues,[33] **1b** and **1c** show extensive N−H···Cl hydrogen bonding in the solid state. The first TACN- and TPM-supported imido vanadium compounds were readily prepared from **1**, and a number of their X-ray structures have been determined. The EPR spectra for **1**−**3** were rather similar but nonetheless did show a small dependence of the *g* values and hyperfine couplings *A* on the nature of the imido nitrogen substituent. The TACN-supported compounds **2** were inactive as ethylene polymerization precatalysts, and the TPM-supported homologues **3** were only moderately active, generally giving PEs with broad molecular weight distributions. The most active catalyst **3b** produced predominately very low M_w PE. These differences in comparison with the highly active TACN- and TPM-supported titanium(4+) analogues are consistent with previous literature reports for vanadocene, CGC, and diamide-based vanadium(4+) catalyst systems. The low (or lack of) activity of the catalysts in general is consistent with previous reports for vanadium-based Ziegler−Natta systems.

Experimental Section

General Methods and Instrumentation. All air- and moisture-sensitive operations were carried out using standard Schlenk-line (Ar) and drybox (N_2) techniques. Protio and deutero solvents were purified, dried, and distilled using conventional techniques. IR spectra were recorded on a Perkin-Elmer Paragon 1000 FT-IR spectrometer as Nujol mulls between NaCl windows and, in some instances, as CH_2Cl_2 solutions using a 0.1-mm-path-length NaCl cell. All data are quoted in wavenumbers (cm^{-1}). Mass spectra were recorded on a Micromass GCT TOF Instrument using a solid probe inlet temperature program. All data are quoted in a mass/charge ratio (*m*/*z*). The X-band (9.450-GHz) EPR spectra were recorded at 120 and 295 K using a commercial Bruker EMX spectrometer. The EPR spectra have been analyzed using commercial Bruker programs WINEPR and XSophie. Polymer characterization was carried out by Rapra Technology. Elemental analyses were carried out by the analytical laboratory of the Inorganic Chemistry Laboratory, University of Oxford, or by the Elemental Analysis Service, London Metropolitan University.

Starting Materials. The compounds V(NMe_2)$_4$,[52] V(N-2,6-$C_6H_3{}^iPr_2$)Cl_2(NHMe_2)$_2$,[33] TACN,[53] and TPM[54] were prepared according to the literature methods. Liquid primary amines and Me_3SiCl were predried over freshly ground CaH_2 and distilled prior to use. All other compounds and reagents were purchased from commercial chemical suppliers and used without further purification.

(52) Bradley, D. C.; Gitlitz, M. H. *J. Chem. Soc. (A)* **1969**, 980.
(53) Madison, S. A.; Batal, D. J. (Unilever PLC, U.K.; Unilever NV). U.S. Patent 5,284,944, 1994, p 21 ff.
(54) Reger, D. L.; Grattan, T. C.; Brown, K. J.; Little, C. A.; Lamba, J. J. S.; Rheingold, A. L.; Sommer, R. D. *J. Organomet. Chem*. **2000**, *607*, 120.

V(NR)Cl_2(NHMe_2)$_2$ (1b−e). (a) General Procedure. To a toluene solution (15 mL) of V(NMe_2)$_4$ (ca. 1−5 mmol) and RNH_2 (1 equiv) at room temperature was slowly added Me_3SiCl (8 equiv). The resulting solution was heated at 100 °C for 16 h. Volatiles were removed and the resulting solids washed with pentane (2 × 10 mL) and dried in vacuo. The target compounds were obtained as analytically pure air- and moisture-sensitive green or brown solids. Full details are provided in the Supporting Information.

(b) Data for 1b (R = 2-$C_6H_4{}^tBu$). Yield: 91%. IR (NaCl plates, Nujol, cm^{-1}): 3583(w), 3255(s), 1584(w), 1401(m), 1293(m), 1092(m), 1047(m), 1014(s), 899(m), 800(m), 761(s), 722(w), 665(w). IR (NaCl cell, CH_2Cl_2, ν(N−H), cm^{-1}): 3289. Anal. Found (calcd for $C_{14}H_{27}Cl_2N_3V$): C, 46.7 (46.8); N, 11.6 (11.7); H, 7.4 (7.6). EI-MS: *m*/*z* 147 (95%; [N-2-$C_6H_4{}^tBu]^+$), 69 (93%; [$^tBu]^+$). FI-MS: *m*/*z* 358 (5%; $[M]^+$), 313 (22%; $[M - NHMe_2]^+$). FI-HRMS for V(N-2-$C_6H_4{}^tBu$)Cl_2(NHMe_2)$_2$. Found (calcd for $C_{14}H_{27}Cl_2N_3V$): 358.1010 (358.1022).

(c) Data for 1c (R = 2-$C_6H_4CF_3$). Yield: 90%. IR (NaCl plates, Nujol, cm^{-1}): 3263(s), 1591(m), 1563(m), 1338(s), 1312(s), 1255(m), 1153(m), 1134(s), 1107(s), 1057(s), 1030(s), 897(m), 800(m), 759(s). IR (NaCl cell, CH_2Cl_2, ν(N−H), cm^{-1}): 3289. Anal. Found (calcd for $C_{11}H_{18}Cl_2F_3N_3V$): C, 35.5 (35.6); N, 11.4 (11.3); H, 5.0 (4.9). FI-MS: *m*/*z* 370 (15%; $[M]^+$), 324 (100%; $[M - NHMe_2 - H]^+$).

(d) Data for 1d (R = ^tBu). Yield: 64%. IR (NaCl plates, Nujol, cm^{-1}): 3235(s), 1613(w), 1401(w), 1358(m), 1238(s), 1212(m), 1122(m), 1091(m), 1029(s), 903(m), 801(m), 722(w), 665(w). IR (NaCl cell, CH_2Cl_2, ν(N−H), cm^{-1}): 3293. Anal. Found (calcd for $C_8H_{23}Cl_2N_3V$): C, 33.9 (33.9); N, 14.8 (14.8); H, 8.1 (8.2). FI-MS: *m*/*z* 282 (7%; $[M]^+$), 248 (7%; $[M - 2Cl]^+$), 236 (45%; $[M - C_3H_9 - H]^+$). FI−HRMS for V(N^{t}Bu)Cl_2(NHMe_2)$_2$. Found (calcd for $C_8H_{23}Cl_2N_3V$): 282.0718 (282.0709).

(e) Data for 1e (R = Ad). Yield: 67%. IR (NaCl plates, Nujol, cm^{-1}): 3293(w), 3233(s), 1599(w), 1302(m), 1224(m), 1115(w), 1099(m), 1026(m), 987(m), 896(m), 843(w), 811(w), 722(w), 665(w). IR (NaCl cell, CH_2Cl_2, ν(N−H), cm^{-1}): 3293. Anal. Found (calcd for $C_{14}H_{29}Cl_2N_3V$): C, 46.7 (46.6); N, 11.7 (11.6); H, 8.0 (8.1). FI-MS: *m*/*z* 360 (3%; $[M]^+$), 314 (15%; $[M - NHMe_2 - H]^+$).

V(NR)(TACN)Cl_2 (2a−e). (a) General Procedure. To a benzene solution (30 mL) of V(NR)Cl_2(NHMe_2)$_2$ (ca. 0.5−2 mmol) was added TACN (1 equiv). The reaction mixture was heated at 80 °C for 3 h then left stirring at room temperature for 16 h. The reaction mixture was filtered and the precipitate washed with benzene (2 × 10 mL) then dried in vacuo. The target compounds were obtained as analytically pure air- and moisture-sensitive green or red solids. Full details are provided in the Supporting Information.

(b) Data for 2a (R = 2,6-$C_6H_3{}^iPr_2$). Yield: 73%. IR (NaCl plates, Nujol, cm^{-1}): 1420(w), 1307(w), 1157(w), 1067(m), 1006(m), 959(w), 890(w), 801(m), 788(m), 759(w). Anal. Found (calcd for $C_{21}H_{38}Cl_2N_4V$): C, 53.8 (53.8); N, 11.9 (12.0); H, 8.2 (8.2). EI-MS: *m*/*z* 467 (7%; $[M]^+$), 292 (3%; $[M - (N\text{-}2,6\text{-}C_6H_3{}^iPr_2)]^+$).

(c) Data for 2b (R = 2-$C_6H_4{}^tBu$). Yield: 44%. IR (NaCl plates, Nujol, cm^{-1}): 1491(w), 1426(m), 1293(w), 1228(w), 1159(w), 1091(m), 1066(m), 1009(s), 951(w), 896(w), 788(m), 771(s). Anal. Found (calcd for $C_{19}H_{34}Cl_2N_4V$): C, 51.7 (51.8); N, 12.7 (12.7); H, 7.9 (7.8). EI-MS: *m*/*z* 439 (10%; $[M]^+$), 292 (4%; $[M - (N\text{-}2\text{-}C_6H_4{}^tBu)]^+$). EI-HRMS for V(N-2-$C_6H_4{}^tBu$)$Cl_2$(TACN). Found (calcd for $C_{19}H_{34}Cl_2N_4V$): 439.1582 (439.1600).

(d) Data for 2c (R = 2-$C_6H_4CF_3$). Yield: 70%. IR (NaCl plates, Nujol, cm^{-1}): 1590(w), 1555(w), 1324(s), 1300(w), 1159(m), 1119(s), 1061(s), 1029(m), 1006(m), 959(w), 895(w), 789(m), 765(w), 682(m). Anal. Found (calcd for $C_{16}H_{25}Cl_2F_3N_4V$): C, 42.4 (42.5);

Table 7. X-ray Data Collection and Processing Parameters for V(N-2-C_6H_4R)Cl_2($NHMe_2$)$_2$ [R = ^{t}Bu (**1b**, Monoclinic and Orthorhombic Diamorphs) or CF_3 (**1c**)], V(N-2-C_6H_4R)(TACN)Cl_2 [R = ^{t}Bu (**2b**) or CF_3 (**2c**)], V(N^{t}Bu)(TACN)Cl_2·CH_2Cl_2 (**2d**·CH_2Cl_2), V(N-2,6-$C_6H_3{}^i$Pr$_2$)(TPM)Cl_2 (**3a**), V(N-2-$C_6H_4{}^t$Bu)(TPM)Cl_2·2.59CH_2Cl_2 (**3b**·2.59CH_2Cl_2), and V(N-2-$C_6H_4CF_3$)(TPM)Cl_2 (**3c**·CH_2Cl_2)

	1b				
	monclinic	orthorhombic	**1c**	**2b**	**2c**
empirical formula	$C_{14}H_{27}Cl_2N_3V$	$C_{14}H_{27}Cl_2N_3V$	$C_{11}H_{18}Cl_2F_3N_3V$	$C_{19}H_{34}Cl_2N_4V$	$C_{16}H_{25}Cl_2F_3N_4V$
fw	359.23	359.23	371.12	440.35	452.24
temp (K)	150	150	150	150	150
wavelength (Å)	0.710 73	0.710 73	0.710 73	0.710 73	0.710 73
space group	*C*2/*c*	*Pbca*	*Pna*2$_1$	*P*2$_1$/*n*	*P*2$_1$/*n*
a (Å)	29.9098(8)	12.8825(2)	16.0311(2)	9.2784(3)	7.4288(2)
b (Å)	6.4650(2)	15.5435(3)	6.4901(2)	14.4815(5)	16.5641(4)
c (Å)	19.8323(6)	19.5799(3)	32.2426(4)	15.9747(7)	15.6021(3)
α (deg)	90	90	90	90	90
β (deg)	101.2391(11)	90	90	98.0961(13)	91.9069(10)
γ (deg)	90	90	90	90	90
V (Å^3)	3761.37(19)	3920.66(11)	3354.63(12)	2125.05(14)	1918.80(8)
Z	8	8	8	4	4
d(calcd) (Mg m^{-3})	1.269	1.217	1.470	1.376	1.565
abs coeff (mm^{-1})	0.807	0.774	0.932	0.729	0.831
R indices: R_1, R_w [$I > 3\sigma(I)$][a]	0.0320, 0.0350	0.0308, 0.0381	0.0347, 0.0351	0.0331, 0.0344	0.0339, 0.0417

	2d·CH_2Cl_2	**3a**	**3b**·2.59CH_2Cl_2	**3c**·CH_2Cl_2
empirical formula	$C_{13}H_{32}Cl_2N_4V$·CH_2Cl_2	$C_{28}H_{39}Cl_2N_7V$·2.59CH_2Cl_2	$C_{26}H_{35}Cl_2N_7V$·CH_2Cl_2	$C_{23}H_{26}Cl_2F_3N_7V$
fw	449.19	595.51	787.10	664.28
temp (K)	150	150	150	150
wavelength (Å)	0.710 73	0.710 73	0.710 73	0.710 73
space group	*Pbca*	*Cc*	*P*$\bar{1}$	*Pbca*
a (Å)	15.1314(2)	17.7339(4)	10.2032(2)	16.2732(2)
b (Å)	14.3736(2)	9.4865(3)	18.9895(2)	16.0207(2)
c (Å)	19.9057(3)	19.4753(5)	20.5245(3)	22.7571(2)
α (deg)	90	90	79.5401(6)	90
β (deg)	90	116.7186(11)	86.8265(6)	90
γ (deg)	90	90	74.5594(6)	90
V (Å^3)	4329.34(11)	2926.55(14)	3796.36(10)	5932.96(12)
Z	8	4	4	8
d(calcd) (Mg m^{-3})	1.378	1.352	1.387	1.487
abs coeff (mm^{-1})	0.956	0.552	0.802	0.741
R indices: R_1, R_w [$I > 3\sigma(I)$][a]	0.0407, 0.0480	0.0387, 0.0412	0.0646, 0.0801	0.0343, 0.0391

[a] $R_1 = \sum||F_o| - |F_c||/\sum|F_o|$; $R_w = \sqrt{\{\sum w(|F_o| - |F_c|)^2/\sum w|F_o|^2}$.

N, 12.4 (12.4); H, 5.4 (5.6). EI-MS: *m*/*z* 451 (100%; [M]$^+$), 292 (5%; [M − (N-2-$C_6H_4CF_3$)]$^+$).

(e) Data for 2d (R = ^{t}Bu). Yield: 61%. IR (NaCl plates, Nujol, cm^{-1}): 1499(m), 1355(m), 1297(m), 1241(m), 1207(w), 1157(w), 1073(m), 1009(s), 895(w), 789(m), 749(w), 687(m). Anal. Found (calcd for $C_{13}H_{30}Cl_2N_4V$): C, 42.8 (42.9); N, 15.3 (15.4); H, 8.2 (8.3). EI-MS: *m*/*z* 363 (83%; [M]$^+$), 292 (100%; [M − N^{t}Bu]$^+$).

(f) Data for 2e (R = Ad). Yield: 42%. IR (NaCl plates, Nujol, cm^{-1}): 1599(w), 1498(w), 1302(m), 1227(m), 1157(w), 1097(m), 1073(m), 1010(m), 991(w), 894(w), 789(m), 749(w), 685(m). Anal. Found (calcd for $C_{19}H_{36}Cl_2N_4V$): C, 51.5 (51.6); N, 12.7 (12.7); H, 8.2 (8.2). EI-MS: *m*/*z* 441 (100%; [M]$^+$), 292 (24%; [M − (N-Ad)]$^+$). EI-HRMS for V(NAd)Cl_2(TACN). Found (calcd for $C_{19}H_{36}Cl_2N_4V$): 441.1745 (441.1757).

V(NR)(TPM)Cl_2 (3a−e). (a) General Synthetic Procedure. To a benzene solution (20 mL) of V(NR)Cl_2($NHMe_2$)$_2$ (ca. 0.5−2 mmol) was added a solution of HC(Me_2pz)$_3$ (1 equiv) in benzene (10 mL). The reaction mixture was heated at 80 °C for 6 h, allowed to cool, and filtered, and the precipitate was washed with benzene (2 × 10 mL). The product was dried in vacuo. The target compounds were obtained as analytically pure air- and moisture-sensitive green or red solids. Full details are provided in the Supporting Information.

(b) Data for 3a (R = 2,6-$C_6H_3{}^i$Pr$_2$). Yield: 43%. IR (NaCl plates, Nujol, cm^{-1}): 1567(m), 1412(m), 1306(m), 1270(m), 1112(w), 1050(m), 977(w), 863(m), 801(m), 761(m), 707(m). Anal. Found (calcd for $C_{28}H_{39}Cl_2N_7V$): C, 56.5 (56.5); N, 16.4 (16.5); H, 6.8 (6.6). EI-MS: *m*/*z* 594 (7%; [M]$^+$), 175 (16%; [N-2,6-$C_6H_3{}^i$Pr$_2$]$^+$). EI-HRMS for V(N-2,6-$C_6H_3{}^i$Pr$_2$)Cl_2(TPM). Found (calcd for $C_{28}H_{39}Cl_2N_7V$): 594.2059 (594.2084).

(c) Data for 3b (R = 2-$C_6H_4{}^t$Bu). Yield: 50%. IR (NaCl plates, Nujol, cm^{-1}): 1567(s), 1417(m), 1307(s), 1269(s), 1165(w), 1090(m), 1046(m), 917(w), 867(m), 820(m), 748(m), 710(m). Anal. Found (calcd for $C_{26}H_{35}Cl_2N_7V$): C, 55.0 (55.0); N, 17.3 (17.3); H, 6.2 (6.2). EI-MS: *m*/*z* 566 (3%; [M]$^+$), 147 (43%; [N-2-$C_6H_4{}^t$Bu]$^+$). EI-HRMS for V(N-2-$C_6H_4{}^t$Bu)Cl_2(TPM). Found (calcd for $C_{26}H_{35}Cl_2N_7V$): 566.1792 (566.1771).

(d) Data for 3c (R = 2-$C_6H_4CF_3$). Yield: 39%. IR (NaCl plates, Nujol, cm^{-1}): 1731(w), 1567(m), 1413(m), 1336(m), 1309(m), 1165(m), 1101(s),1027(s), 912(w), 860(m), 799(s), 768(m), 701(w), 665(w). Anal. Found (calcd for $C_{23}H_{26}Cl_2F_3N_7V$): C, 47.7 (47.7); N, 16.9 (16.9); H, 4.5 (4.5). EI-MS: *m*/*z* 579 (5%; [M − H]$^+$).

(e) Data for 3d (R = ^{t}Bu). Yield: 55%. IR (NaCl plates, Nujol, cm^{-1}): 1565(s), 1417(m), 1304(s), 1234(m), 1209(w), 1106(m),

1045(s), 913(m), 861(m), 804(m), 703(m), 681(m), 665(w). Anal. Found (calcd for $C_{20}H_{31}Cl_2N_7V$): C, 49.0 (48.9); N, 19.8 (19.9); H, 6.2 (6.4).

(f) Data for 3e (R = Ad). Yield: 46%. IR (NaCl plates, Nujol, cm^{-1}): 3090(w), 1567(s), 1417(s), 1393(s), 1311(s), 1304(s), 1273(s), 1203(w), 1099(m), 1045(s), 987(w), 913(m), 869(m), 861(m), 827(m), 712(m), 677(s). Anal. Found (calcd for $C_{26}H_{37}Cl_2N_7V$): C, 54.9 (54.8); N, 17.3 (17.2); H, 6.6 (6.6). EI-MS: *m*/*z* 384 (5%; $[M - Cl - N\text{-}C_{10}H_{15}]^+$), 298 (7%; $[HC(Me_2pz)_3]^+$).

Polymerization Procedures. To a glass Büchi 1-L autoclave was added MAO (5 mL, 10% in toluene (w/w), 7.5 mmol) made up to 200 mL with toluene. The solution was stirred at 1000 rpm for 5 min. The precatalyst (5 μmol) was dissolved in toluene (50 mL), added to the reactor, and activated by stirring with the MAO solution for 30 min at 1000 rpm. The reaction vessel was placed under full vacuum for 10 s, the stirring was increased to 1500 rpm, and the reactor was placed under a dynamic pressure of 6 bar of ethylene. After 30 min, the autoclave was isolated and the pressure was released. A total of 5 mL of methanol was added, followed by 50 mL of water (with stirring). The mixture was acidified to pH 1 using a solution of 10% HCl in methanol and stirred for 1 h. The precipitated polymers were filtered, washed with water (1000 mL), and dried to constant weight at room temperature.

Crystal Structure Determinations of V(N-2-C_6H_4R)Cl_2-($NHMe_2$)$_2$ [R = ^{t}Bu (1b, Monoclinic and Orthorhombic Diamorphs) or CF_3 (1c)], V(N-2-C_6H_4R)(TACN)Cl_2 [R = ^{t}Bu (2b) or CF_3 (2c)], V(N^{t}Bu)(TACN)Cl_2·CH_2Cl_2 (2d·CH_2Cl_2), V(N-2,6-$C_6H_3{}^i$Pr$_2$)(TPM)Cl_2 (3a), V(N-2-$C_6H_4{}^t$Bu)(TPM)Cl_2·2.59CH_2Cl_2 (3b·2.59CH_2Cl_2), V(N-2-$C_6H_4CF_3$)(TPM)Cl_2·CH_2Cl_2 (3c·CH_2Cl_2), and V(NAd)(TPM)Cl_2·2CH_2Cl_2 (3e·2CH_2Cl_2). Crystal data collection and processing parameters are given in Table 7. Crystals were mounted on glass fibers using perfluoropolyether oil and cooled rapidly in a stream of cold N_2 using an Oxford Cryosystems CRYOSTREAM unit. Diffraction data were measured using an Enraf-Nonius Kappa CCD diffractometer. Intensity data were processed using the DENZO-SMN package.[55] The structures were solved using the direct methods program SIR92,[5656] which located all non-hydrogen atoms. Subsequent full-matrix least-squares refinement was carried out using the CRYSTALS program suite.[57] Coordinates and anisotropic thermal parameters of all non-hydrogen atoms were refined (see additional comments below). Hydrogen atoms bonded to carbon were placed geometrically, while the N−H atoms were located from Fourier difference maps and refined isotropically. However, for the purposes of geometric comparisons with literature compounds such as Ti(NR)Cl_2($NHMe_2$)$_2$, geometric N−H placement using a distance of 0.87 Å was used (see Table 1). Weighting schemes and other corrections were applied as appropriate. For **2b**−**d**, the displacement parameters of the carbon atoms of the triazacyclononane ring were abnormally large and highly anisotropic, which was taken as evidence of disorder. In each case, a second conformation of the ring was identified using difference Fourier maps. Coordinates, anisotropic thermal parameters, and site occupancies were refined for the disordered carbon atoms. Similarity restraints were applied to the lengths of chemically similar bonds [standard uncertainty (su) 0.02 Å] and to chemically similar angles (su 2°), assuming the ring to have regular threefold rotational symmetry. Similarity restraints were also applied to the thermal parameters of directly bonded pairs of atoms. The site occupancy factor for the major and minor orientations were as follows: 0.659 and 0.341 (**2b**); 0.780 and 0.220 (**2c**); 0.695 and 0.305 (**2d**). For **3b**, the coordinates, isotropic displacement parameters, and site occupancies of the carbon and chlorine atoms of the disordered solvent molecules were refined subject to restraint of the C−Cl bond lengths to 1.77(2) Å and of the Cl−C−Cl angles to 112(2)°. Similarity restraints were applied to the displacement parameters of directly bonded pairs of atoms. The high values of the minimum and maximum residual electron densities suggest that the model does not fully agree with the diffraction data. Because the minima and maxima lie close to the chlorine atoms of the disordered solvent, the disagreement is presumed to be due to an oversimplified model of the disorder and to be of no chemical significance. For **3e**, it was clearly apparent that the Ad group was disordered, and this was modeled as being due to disorder over two positions related by the local mirror plane of the {V(TPM)-Cl_2} moiety. Coordinates, anisotropic thermal parameters, and site occupancies were refined for the disordered carbon atoms, subject to restraint of chemically equivalent bond lengths and angles to their common means (su's 0.02 Å and 2°, respectively). A difference Fourier map showed the presence of a further molecule of solvent, which was disordered over two orientations. The coordinates, anisotropic displacement parameters, and site occupancies of its carbon and chlorine atoms were refined subject to restraint of the C−Cl bond lengths to 1.77(2) Å and the Cl−C−Cl angles to 112(2)°.

A full listing of atomic coordinates, bond lengths and angles, and displacement parameters for all of the structures has been deposited at the Cambridge Crystallographic Data Center (12 Union Road, Cambridge CB2 1EZ, U.K., tel +44 1223 336408, fax +44 1223 336033).

Acknowledgment. We thank EPSRC and DSM Research for support.

Supporting Information Available: X-ray crystallographic data in CIF format for the structure determinations of **1b** (two diamorphs), **1c**, **2b**, **2c**, **2d**·CH_2Cl_2, **3a**, **3b**·2.59CH_2Cl_2, **3c**·CH_2Cl_2, and **3e**·2CH_2Cl_2, full synthetic procedures for compounds **1b**−**e**, **2a**−**e**, and **3a**−**e**, further cell packing diagrams for **1b** and **1c**, plots of the orthorhombic form of **1b** and the other crystallographically independent molecules of **1c** and **3b**, and ethylene uptake traces. This material is available free of charge via the Internet at http://pubs.acs.org.

IC060454I

(55) Otwinowski, Z.; Minor, W. *Processing of X-ray Diffraction Data Collected in Oscillation Mode*; Academic press: New York, 1997.
(56) Altomare, A.; Cascarano, G.; Giacovazzo, G.; Guagliardi, A.; Burla, M. C.; Polidori, G.; Camalli, M. *J. Appl. Crystallogr.* **1994**, *27*, 435.
(57) Betteridge, P. W.; Cooper, J. R.; Cooper, R. I.; Prout, K.; Watkin, D. J. *J. Appl. Crystallogr.* **2003**, *36*, 1487.